DOI: 10.1002/ejic.200600449

New Multidimensional Coordination Polymers with μ_2- and μ_3-dcno Cyano Carbanion Ligand {dcno$^-$ = [(NC)$_2$CC(O)O(CH$_2$)$_2$OH]$^-$}

Samia Benmansour,[a,b] Fatima Setifi,[a][‡] Smail Triki,*[a] Jean-Yves Salaün,[a]
Fanny Vandevelde,[a] Jean Sala-Pala,[a] Carlos J. Gómez-García,*[b] and Thierry Roisnel[c]

Keywords: Cyano carbanions / Bridging ligands / Coordination polymers / Multidimensional networks / Magnetic properties

New polymeric materials [M(dcno)$_2$(H$_2$O)$_2$] [M = Fe^{II} (**1**), Co^{II} (**2**)] and [M(dcno)$_2$] [M = Cu^{II} (**3**), Mn^{II} (**4**)] with dcno$^-$ = [(NC)$_2$CC(O)O(CH$_2$)$_2$OH]$^-$ = 2,2-dicyano-1-(2-hydroxyethoxy)ethenolate anion have been synthesised and characterised by IR spectroscopy, X-ray crystallography and magnetic measurements. In compounds **1** and **2**, each organic ligand acts in a bridging mode with its two nitrogen atoms bound to two different metal ions, while in compounds **3** and **4**, each organic anion acts as a μ_3-bridging ligand through its two nitrogen atoms and the oxygen atom of the OH group. Each metal ion has a pseudo-octahedral *trans*-MN$_4$O$_2$ environment with four nitrogen atoms from four different organic ligands and two oxygen atoms from two water molecules in compounds **1** and **2** and from the OH group of the cyanocarbanion ligand in compounds **3** and **4**. These coordination modes give rise to 1D, 2D and 3D arrangements for compounds **1**, **2** and **3**–**4**, respectively. Magnetic measurements show weak antiferromagnetic coupling between metal centres in the four compounds.

Introduction

Cyano carbanions and cyano azacarbanions are interesting ligands for the preparation of a large variety of discrete and extended molecular structures due to the fact that their cyano groups are disposed in such a way that they cannot coordinate to the same metal ion and that association of the π-electronic system of the nitrile groups with the π-system of the central fragment induces an electronic delocalisation that facilitates transmission of electronic effects between the metal centres (Scheme 1).[1,2]

Thus, reaction of such anions with d-block transition-metal ions leads to the isolation of a variety of new compounds displaying rich structural topological features and unusual magnetic properties;[3–16] most of them concern those involving the simplest anions such as the dicyanamide and the tricyanomethanide anions (dca$^-$ and tcm$^-$, respectively).[3–9] In this regard, binary (dca)metal and (tcm)metal complexes, M(dca)$_2$ and M(tcm)$_2$ (M = Cr^{II}, Mn^{II}, Fe^{II}, Co^{II}, Ni^{II} and Cu^{II}), built from tricoordinate dca and tcm ligands exhibit 3D rutile-like architectures and some of them show long-range magnetic ordering, hard magnetic behaviour or spin-canted antiferromagnetism.[4,5] In addition to these binary dca and tcm compounds, a few binary examples involving sophisticated cyano carbanions and cyano azacarbanions have been reported by others and us.[11–15] Obviously, in these compounds, structural and physical properties are greatly affected by the number of donor groups and by the nature of the central fragment of the anionic ligand; we therefore find it interesting to study new ligands involving two cyano groups, as in the dca ligand, as well as one oxygen atom able to act as a donor or to participate in hydrogen bonds. Thus, using the 2,2-dicyano-1-ethoxyethenolate anion (dcne$^-$) and its methyl analogue (dcnm$^-$) (Scheme 1) led us and Kremer et al. to new compounds whose structures are built from monodimensional chains of 12-membered dimetallacycles.[11,12] These studies showed that the terminal oxygen atom does not enter in the coordination sphere of the metal ion, as the negative charge of the [(NC)$_2$CC(O)OR]$^-$ anion is not mainly located on this terminal oxygen atom. In an effort to increase the dimensionality of the structural arrangements as observed in the dicyanamide binary systems having a rutile-like structure, we have prepared the dcno$^-$ anion, where an –O(CH$_2$)$_2$OH group replaces the –OEt group of the dcne$^-$ anion. This can affect the electronic delocalisation of the whole ligand and modify the role of the terminal oxygen atoms of the organic ligand and, therefore, its coordination mode around the metal ion. Herein, we report the syntheses, structural characterisation and magnetic properties of new polymeric compounds of formula [M(dcno)$_2$(H$_2$O)$_2$]

---

[a] UMR 6521 CNRS – Université de Bretagne Occidentale,
B. P. 809, 29285 Brest Cedex, France
E-mail: triki@univ-brest.fr
[b] ICMol, Universidad de Valencia, Edificio Institutos de Paterna,
P. O. Box 22085, 46071 Valencia, Spain
[c] UMR 6226 CNRS – Université de Rennes
1 Ave du Gal Leclerc, 35042 Rennes Cedex, France
[‡] Permanent address: Département de Chimie, Faculté des Sciences, Université Ferhat-Abbas, Sétif 19000, Algeria

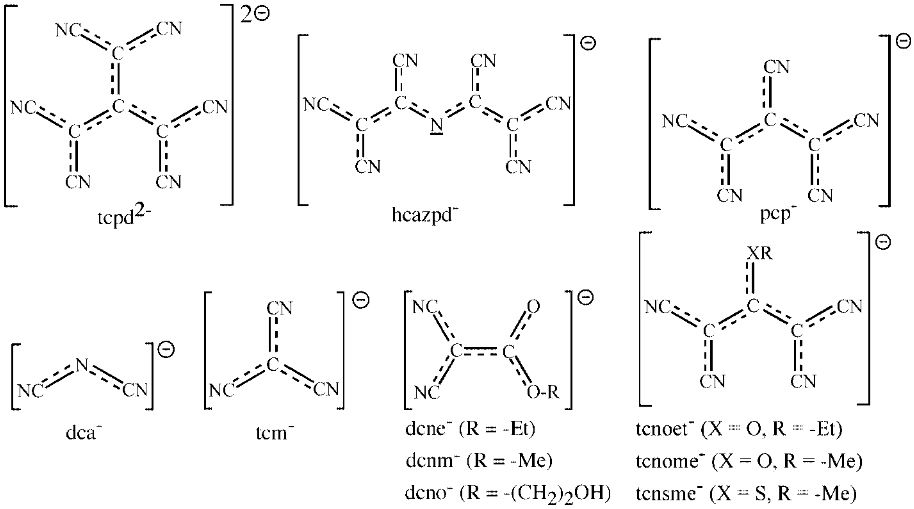

Scheme 1.

[M = Fe^{II} (**1**), Co^{II} (**2**)] and [M(dcno)$_2$] [M = Cu^{II} (**3**), Mn^{II} (**4**)] containing the bridging 2,2-dicyano-1-(2-hydroxyethoxy)ethenolate anion {dcno$^-$ = [(NC)$_2$CC(O)O(CH$_2$)$_2$-OH]$^-$}.

Results and Discussion

Syntheses and Characterisation

Silver 2,2-dicyano-1-(2-hydroxyethoxy)ethenolate [Ag(dcno)] was prepared by smooth hydrolysis of 2-(1,3-dioxolan-2-ylidene)malononitrile in the presence of an excess of silver nitrate; the pH of the aqueous solution (initial value: 6.5) decreased to 1.0 after boiling the solution for a few minutes in agreement with the reaction in Scheme 2. The tetraethylammonium salt was obtained as a white powder by reaction with 1 equiv. of [(C$_2$H$_5$)$_4$N]Cl. Its ^{13}C NMR spectrum (see Experimental Section) is in good agreement with the proposed structure. However, it is worth noting the presence of a single signal for the two nonequivalent C≡N groups. This observation suggests a fast rotation, compared to the NMR detection around the central "C=C" bond resulting from an efficient electron delocalisation along the molecule induced by the presence of the two electron-withdrawing C≡N groups. Treatment of a saturated solution of Ag(dcno) with a saturated aqueous solution of the corresponding metal salt (MCl$_2$·nH$_2$O) in a dcno$^-$/M^{II} ratio of 2 gave, after slow concentration, the new compounds [M(dcno)$_2$(H$_2$O)$_2$] [M = Fe^{II} (**1**), Co^{II} (**2**)] and [M(dcno)$_2$] [M = Cu^{II} (**3**), Mn^{II} (**4**)]. All compounds can also be prepared in the same way as the silver salt by direct reaction in aqueous solution of 2-(1,3-dioxolan-2-ylidene)malononitrile with the corresponding transition-metal salt (Scheme 2).

The IR spectra of compounds **1**–**4** show similar patterns with two strong absorption bands assigned to ν_{CN}. In agreement with the coordination of the organic ligand through its nitrile groups, these bands are slightly shifted to higher wavenumbers (2190–2260 cm^{-1}) than those of the corresponding tetraethylammonium salt containing the uncoordinated dcno$^-$ moiety (2169–2197 cm^{-1}).

Crystal Structures

The two compounds of formula [M(dcno)$_2$(H$_2$O)$_2$] [M = Fe^{II} (**1**), Co^{II} (**2**)] display two different structures although generated by similar asymmetric units consisting of a metal ion and a water molecule, both on special positions [(0,–y,3/4) and (0,0,0) for **1** and **2**, respectively], and one dcno$^-$ organic ligand located on a general position. Each metal ion is linked to four nitrogen atoms from four organic ligands and to two symmetrically equivalent water molecules in a *trans* configuration.

In compound **1**, the coordination sphere of the metal atom can be described as a noncentrosymmetric *trans*-FeN$_4$O$_2$ pseudo-octahedron formed by an FeN$_4$ plane, arising from four nitrogen atoms (N1$^{(b)}$, N1$^{(c)}$, N2, N2$^{(a)}$), and two water molecules (O4 and O4$^{(a)}$) in axial positions (Figure 1). The six bond lengths are almost equivalent [ranging from 2.137(3) to 2.141(4) Å]. The structure involves 12-membered [Fe(NCCCN)$_2$Fe] dimetallacycles, as two bridging dcno$^-$ ligands connect two Fe^{II} ions (Figure 1). These

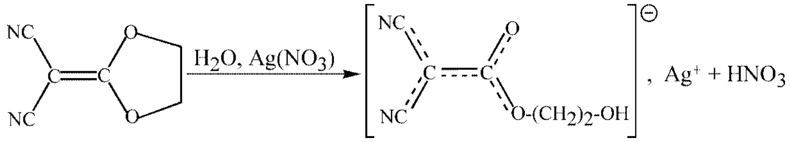

Scheme 2.

almost planar rings (larger deviation from the corresponding mean plane of 0.04 Å) share metal ions to give a chain of dimetallacycles running along the [010] direction (Figure 1).

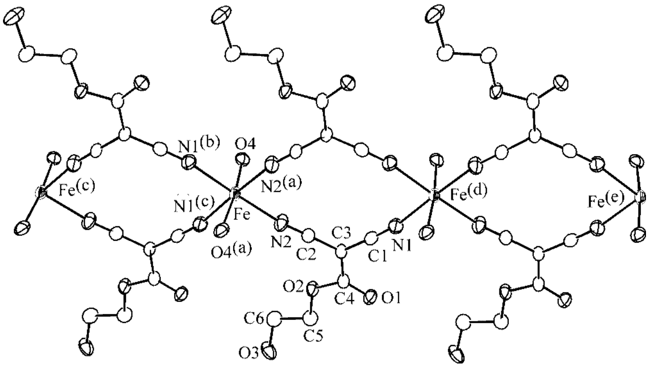

Figure 1. ORTEP perspective view of **1** (50% probability ellipsoid) showing the atom-labelling scheme, the Fe^{II} environment and the 1D structure generated by the μ_2-dcno ligand. Codes of equivalent positions: (a) 1 – *x*, *y*, 3/2 – *z*; (b) 1 – *x*, –1 + *y*, 3/2 – *z*; (c) *x*, –1 + *y*, *z*; (d) *x*, 1 + *y*, *z*; (e) *x*, 2 + *y*, *z*.

The intrachain Fe···Fe distance [7.450(1) Å], slightly shorter than the shortest interchain one [7.8660(6) Å], is close to that observed in the iron–dicyanamide compounds $[Fe(dca)_2(CH_3OH)_2]$[4d] and {[Fe(4,4′-bpy)(dca)$_2$]·bt}[16] (bt = 2,2′-bithiazoline) involving similar chains [7.392(1) and 7.418(1) Å, respectively].

In compound **2** each metal ion has a *trans*-CoN_4O_2 octahedral environment formed by four nitrogen atoms from four organic ligands (N1, N1$^{(a)}$, N2$^{(b)}$ and N2$^{(c)}$) and two equivalent water molecules (O4 and O4$^{(a)}$) (Figure 2a); this environment, essentially similar to that observed in compound **1**, is centrosymmetric here. As in **1**, the organic ligand acts in a bridging mode, with its two nitrogen atoms, N1 and N2, bound to two different cobalt ions (Figure 2a); but here the coordination mode leads to a two-dimensional structure, as the four organic ligands of one $[Co(dcno)_4]$ fragment are linked to four different Co^{II} ions (Figure 2b). Thus, the two structures **1** and **2**, despite their essentially equivalent asymmetric units, display two very different molecular arrangements.

As shown in Figure 2b, the 2D layers of **2** can be described as formed by a succession of nonplanar [Co(NCCCN)Co(NCCCN)Co(NCCCN)Co(NCCCN)] cycles; these 24-membered tetrametallacycles are of course clearly different from the essentially planar 12-membered dimetallacycles described above for compound **1**. The shortest intramolecular Co···Co distance [7.929(1) Å] is shorter than that observed between the adjacent layers [8.421(1) Å]. This relatively long interlayer distance can be explained by the steric effects due to the nonplanar metallacycles, as clearly shown in Figure 2c. Careful examination of the interlayer distances reveals the presence of hydrogen bonds between the coordinated water molecule (O4) and the oxygen atom of the $–(CH_2)_2OH$ group of the dcno$^–$ ligand (O3) [O3···O4 2.81(1) Å]. This gives rise to the overall 3D structure depicted in Figure 2c.

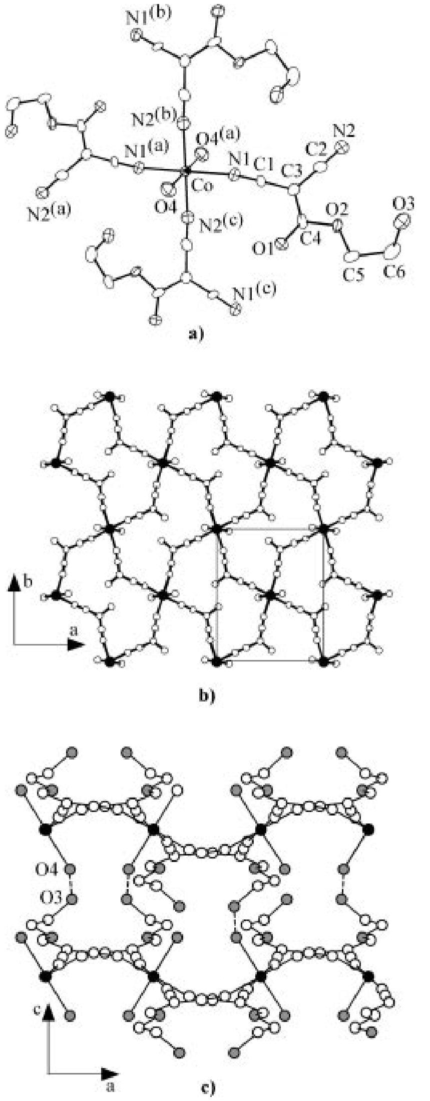

Figure 2. Structure of **2**. a) ORTEP perspective view (50% probability ellipsoid) showing the atom-labelling scheme and the Co^{II} environment. Codes of equivalent positions: (a) –*x*, –*y*, –*z*; (b) –1/2 – *x*, 1/2 + *y*, *z*; and (c) 1/2 + *x*, –1/2 – *y*, –*z*. b) Two-dimensional structure in the *ab* plane; noncoordinated groups [–O and $–OCH_2CH_2OH$] omitted for clarity. c) Projection of two adjacent 2D layers in the *ac* plane showing hydrogen bonds in **2** [O3···O4 2.81(1) Å]. Shortest interlayer Co···Co distance: 8.421(1) Å.

Compounds **3** and **4** are isostructural. In both cases, the asymmetric unit contains a metal ion located on a special position (0,0,0) and a dcno$^–$ ligand on a general position (Figure 3). Each metal ion has a centrosymmetric *trans*-MN_4O_2 distorted octahedral environment formed by an MN_4 plane arising from four nitrogen atoms (N1, N1$^{(a)}$, N2$^{(c)}$ and N2$^{(e)}$) of four organic ligands, and two oxygen atoms from OH groups (O3$^{(b)}$ and O3$^{(d)}$) of two other dcno$^–$ ligands (Figure 3). Thus, in contrast to compounds **1** and **2**, here the metal ions are linked to six organic ligands.

Examination of the crystallographic data depicted in Table 1 reveals that the Cu^{II} octahedral environment of compound **3** is much more distorted than that of the Mn^{II}

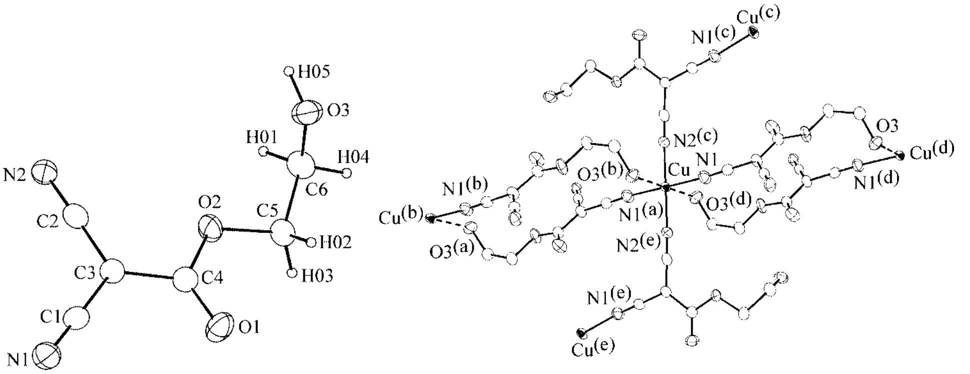

Figure 3. Structure of **3** and **4**. ORTEP view of **3** (50% probability ellipsoid) showing the atom-labelling scheme and the Cu^{II} environment. M···M distances [Å] in **3**: Cu···Cu$^{(c)}$ 7.5648(4), Cu···Cu$^{(b)}$ 10.1242(4); in **4**: Mn···Mn$^{(c)}$ 7.740(5), Mn···Mn$^{(b)}$ 10.264(5). Codes of equivalent positions: (a) $-x, -y, -z$; (b) $x, y, -1 + z$; (c) $1/2 - x, -1/2 + y, 1/2 - z$; (d) $-x, -y, 1 - z$; (e) $-1/2 + x, 1/2 - y, -1/2 + z$.

ion in **4**, as the six metal–ligand bond lengths in **4** are almost equivalent [from 2.197(2) to 2.230(2) Å], while in the Cu compound **3**, the CuN$_4$ equatorial plane involves four essentially equivalent Cu–N bond lengths [1.995(2) and 1.998(2) Å], which are significantly shorter than the two axial Cu–O ones [2.359(2) Å]. These bond lengths clearly show the presence of Jahn–Teller distortions, as usually observed in octahedral Cu^{II} complexes. The coordination mode of the dcno$^-$ ligand is different from that observed for compounds **1** and **2**, as, here, this ligand acts as a μ_3-bridging ligand through its two nitrogen atoms (N1 and N2) and its oxygen atom (O3) of the OH group (Figure 3), leading to the overall three-dimensional structure depicted in Figure 4b.

Table 1. Selected bond lengths [Å] and bond angles [°] in compounds **1**–**4**.

	1	**2**	**3**	**4**
M–N1	2.141(4)	2.104(7)	1.998(2)	2.230(2)
M–N2	2.137(3)	2.083(8)	1.995(2)	2.197(2)
M–O4	2.141(3)	2.144(5)		
M–O3			2.359(2)	2.197(2)
N1–C1	1.153(5)	1.15(1)	1.141(3)	1.144(2)
N2–C2	1.143(5)	1.17(1)	1.145(3)	1.145(2)
C1–C3	1.393(6)	1.39(1)	1.408(4)	1.409(2)
C2–C3	1.408(6)	1.40(1)	1.396(4)	1.399(2)
C3–C4	1.434(6)	1.43(1)	1.442(4)	1.433(2)
C4–O1	1.221(5)	1.23(1)	1.220(3)	1.222(2)
C4–O2	1.345(5)	1.345(9)	1.334(3)	1.346(2)
C5–C6	1.485(7)	1.50(1)	1.494(4)	1.498(2)
C5–O2	1.441(5)	1.45(1)	1.463(3)	1.448(2)
C6–O3	1.422(5)	1.45(1)	1.430(4)	1.435(2)
N1–C1–C3	177.2(4)	178.0(9)	179.2(3)	177.3(2)
N2–C2–C3	178.2(4)	177.3(9)	178.4(3)	179.2(2)
C1–C3–C2	118.5(4)	118.5(7)	118.3(2)	118.0(1)
C1–C3–C4	121.0(4)	122.7(7)	120.1(2)	120.5(1)
C2–C3–C4	120.4(4)	118.8(8)	121.6(2)	121.5(1)
C3–C4–O1	125.2(4)	126.9(7)	124.4(2)	125.8(1)
C3–C4–O2	111.3(3)	111.1(8)	111.0(2)	110.8(1)
O1–C4–O2	123.6(4)	122.0(7)	124.6(2)	123.5(1)
C4–O2–C5	118.6(3)	118.5(6)	117.4(2)	117.6(1)
O2–C5–C6	105.7(3)	106.4(7)	106.9(2)	106.6(1)
C5–C6–O3	108.4(4)	111.6(6)	110.2(2)	110.5(1)
N1–M–N1	88.2(1)	180.00	180.00	180.00
N1–M–N2	93.3(1)	90.0(3)	92.17(9)	93.77(4)
N1–M–N2	177.7(1)	90.0(3)	87.83(9)	86.23(4)
N2–M–N2	85.4(1)	180.00	180.00	180.00
N1–M–O4	87.1(1)	88.9(3)		
N1–M–O4	89.0(1)	91.1(3)		
N1–M–O3			90.53(9)	90.70(5)
N1–M–O3			89.47(9)	89.30(5)
N2–M–O4	94.7(1)	90.9(3)		
N2–M–O4	89.3(1)	88.9(3)		
N2–M–O3			90.49(8)	91.06(4)
N2–M–O3			89.51(8)	88.94(4)
O4–M–O4	174.6(1)	180.00		
O3–M–O3			180.00	180.00

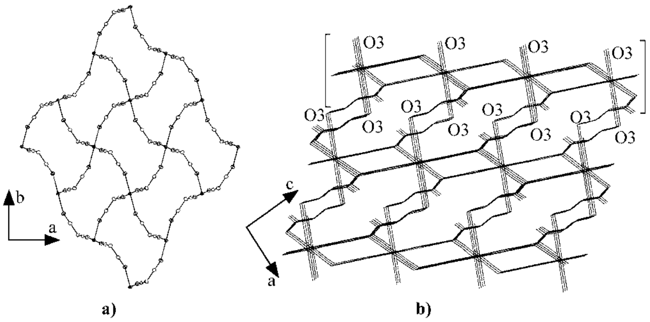

Figure 4. Sophisticated three-dimensional structure of **3** and **4**. a) 2D motif generated by the C(CN)$_2$ fragment in **3**; –C(O)(OCH$_2$-CH$_2$OH) group of the dcno$^-$ ligand omitted for clarity. b) 3D structure of **3** showing the 2D motifs linked through the OH group (O3 atom) of the dcno$^-$ ligand.

The shortest M^{II}···M^{II} distance through the dcno$^-$ ligand corresponds to that observed between two metal ions linked by the C(CN)$_2$ fragment [Cu···Cu$^{(c)}$ 7.5648(4) Å; Mn···Mn$^{(c)}$ 7.740(5) Å]; whereas the M^{II}···M^{II} distance observed through the NCCCO(CH$_2$)$_2$OH fragment (see Figure 3) is significantly longer [Cu···Cu$^{(b)}$ 10.1242(4) Å; Mn···Mn$^{(b)}$ 10.264(5) Å] (Figure 4b). It is worth noting that the best way to describe this complicated 3D molecular arrangement is to consider the 2D elemental unit generated by the μ_2-C(CN)$_2$ fragment as shown in Figure 4a. These layers are connected to each other through the M^{II}–O3 bridges leading to the 3D structure of **3** and **4**.

Examination of bond lengths and bond angles clearly shows that the crystallographic parameters of the dcno$^-$ ligand are not significantly different in compounds **1**–**4** (Table 1 and Figure 3). With the exception of the

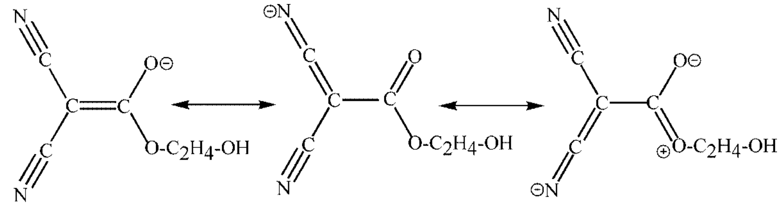

Scheme 3.

"–CH_2CH_2OH" group, the organic ligand is essentially planar within a maximum deviation of 0.06 Å from the corresponding mean plane. This is in agreement with an sp^2 hybridisation of the two central carbon atoms (C3 and C4), also shown by the bond angles around these atoms in each compound (sums of bond angles around C3 and C4 range from 359.9 to 360.1°), associated with an sp hybridisation of the carbon atoms of the cyano groups. Crystallographic data depicted in Table 1 for these compounds clearly show that the cyanocarbanion ligand includes a highly delocalised conjugated system. The electronic delocalisation is clearly shown by (i) a rather short terminal C4–O1 bond (1.22–1.23 Å) that strongly deviates from a normal C–O single bond (1.50 Å); (ii) a central C3–C4 bond (1.43–1.44 Å) longer than a normal C=C double bond (1.34 Å) [this low double-bond character is in good agreement with the ^{13}C NMR spectrum, as only a single signal was observed for the two C≡N groups of the free $dcno^-$ anion (see Experimental Section)]; and (iii) two C–CN bonds (1.39–1.41 Å) and a C4–O2 bond (1.33–1.35 Å), all presenting some multiple character. These observations indicate that the bonding in the $dcno^-$ ligand cannot be explained by a simple Lewis structure; this organic ligand must be considered as a resonance hybrid of different canonical structures (Scheme 3).

These canonical forms, and their symmetrical ones (not shown in Scheme 3), give rise to the mean electronic structure of Scheme 4, in agreement with the planarity of the $[(NC)_2CC(O)O]$ group and with the structural data (Table 1). Thus, it is clear that in this ligand the negative charge is not mainly located on the terminal oxygen atom and therefore, as also observed in the $dcne^-$ anion (Scheme 1),[11] it is not surprising that this atom does not enter in the coordination sphere of the metal ion.

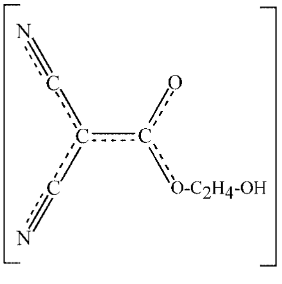

Scheme 4.

Magnetic Properties

The thermal variation of the product of the molar susceptibility times the temperature ($\chi_M T$) for compound **1** shows a room-temperature value of 3.2 emu K mol^{-1}. When cooling down, $\chi_M T$ remains constant to about 30 K, where a progressive decrease is observed, to reach a value of about 0.6 emu K mol^{-1} at 2 K (Figure 5).

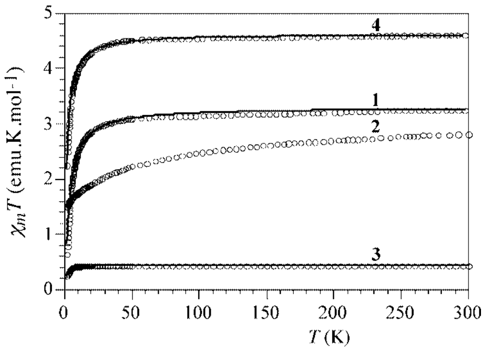

Figure 5. Thermal variation of $\chi_M T$ for compounds **1**–**4**. Solid lines represent the best fit to the models (see text).

Compound **2** shows a room-temperature $\chi_M T$ value of 2.8 emu K mol^{-1} and a continuous decrease when the temperature is lowered, reaching a value of about 1.5 emu K mol^{-1} at 2 K (Figure 5).

Finally, compounds **3** and **4** show a similar behaviour to that of compound **1**: they present room-temperature $\chi_M T$ values of 0.4 and 4.6 emu K mol^{-1}, respectively, which remain constant down to about 15 K (for **3**) and about 50 K (for **4**), where a progressive decrease is observed in both compounds, reaching values at 2 K of 0.2 and 2.2 emu K mol^{-1}, respectively. In compounds **1**, **3** and **4** the room-temperature $\chi_M T$ values are very close to the expected ones for high-spin Fe^{II} ($S = 2$), Cu^{II} ($S = 1/2$) and Mn^{II} ($S = 5/2$) ions with spin-only contribution (3.0, 0.375 and 4.375 emu K mol^{-1}, respectively). In compound **2**, the $\chi_M T$ value (2.8 emu K mol^{-1}) is in the range of the observed values for high-spin octahedral monomeric Co^{II} ions (2.7–3.4 emu K mol^{-1}), where a significant orbital contribution is expected due to its orbitally degenerated $^4T_{1g}$ ground state.[17] The decrease observed at high temperatures in compound **2** is due to the presence of spin-orbit coupling, as expected for paramagnetic Co^{II} compounds.[18] In compounds **1**, **3** and **4**, the decrease observed in $\chi_M T$ at low temperatures can be attributed to the presence of weak, although noticeable, antiferromagnetic interactions. Note that for compounds **1** and **4** we cannot exclude the presence of a zero-field splitting (ZFS), which may also account for the decrease observed in $\chi_M T$ at low temperatures. Note also that the decrease observed in compound **3** (where no ZFS is to be expected) and the structural similarities in all compounds (same kind of –NC–C–CN– bridges between metal centres) indicate that the ZFS cannot be the only reason for the decrease in χ_MT at low temperatures and, therefore, that there must be a weak antiferromagnetic coupling in all cases. Furthermore, although the attempts to fit the χ_MT product for compounds **1** and **4** to isolated monomers with ZFS satisfactorily reproduce the magnetic properties in the whole temperature range, the $|D|$ values obtained are unrealistically high (above 16 and 10 K for **1** and **4**, respectively), confirming the presence of a weak, although not negligible, antiferromagnetic coupling.

From the structural data that show the presence of a chain of dimetallacycles in compound **1**, we have reproduced the magnetic behaviour of **1** with the model derived by Fisher for a regular antiferromagnetic chain (with S = 2 in compound **1**);[19] N is the Avogadro number, k is the Boltzmann constant and β is the Bohr magneton.

$$\chi_M = \frac{Ng^2\beta^2S(S+1)}{3kT}\left[\frac{1+u}{1-u}\right], \text{ where } u = \coth\left[\frac{JS(S+1)}{kT}\right] - \left[\frac{kT}{JS(S+1)}\right]$$

This model very satisfactorily reproduces the magnetic behaviour of compound **1** in the whole temperature range (solid line in Figure 5) with g = 2.094(3) and J = –0.78(1) K = –0.54(1) cm^{-1} (the Hamiltonian is written as $H = -J\,\Sigma S_iS_{i+1}$).

In compounds **3** and **4** the structure shows the presence of a 2D lattice with identical exchange pathways (NC–C–CN) in the two directions and an extra connection through a very long NCCC(O)(CH_2)$_2$OH bridge. In a first approximation we can consider that the magnetic exchange is mainly due to the shorter NC–C–CN bridges and, accordingly, we have used the antiferromagnetic square 2D model (Quadratic Layer Antiferromagnet) proposed by Lines[20] to reproduce the magnetic data of these compounds:

$$\chi_M = \frac{Ng^2\beta^2}{J}\left(3\theta + \sum_n \frac{C_n}{\theta^{n-1}}\right)^{-1}, \text{ where } \theta = \frac{kT}{JS(S+1)}$$

The six first C_n coefficients are: 4.0, 2.667, 1.185, 0.149, –0.191 and 0.001 for S = 1/2 (compound **3**) and 4.0, 1.448, 0.228, 0.262, 0.119 and 0.017 for S = 5/2 (compound **4**). This model very satisfactorily reproduces the magnetic behaviour of compounds **3** and **4** in the whole temperature range (solid lines in Figure 5) with g = 2.195(3) and J = –0.92(3) K = –0.64(2) cm^{-1} for **3** and g = 2.054(1) and J = –0.128(1) K = –0.089(1) cm^{-1} for **4** (the Hamiltonian is written as $H = -J\,\Sigma S_iS_j$).

These results indicate that the antiferromagnetic coupling is very weak in the three compounds, as expected from the presence of identical M–NC–C–CN–M bridges, and that the long bridges present in the structures of compounds **3** and **4** do not play an important role in the magnetic interactions. Furthermore, the J values are very similar to those obtained in the related family of compounds [M(dcne)$_2$(H_2O)$_2$] and [Cu(dcne)$_2$(H_2O)], where similar NC–C–CN bridges are present.[11] An additional confirmation of the weak antiferromagnetic interactions in the four compounds is provided by the isothermal magnetisation measurements at 2 K. These measurements show in each case a behaviour close to that expected for isolated magnetic centres and can be well reproduced with the Brillouin function but with lower g values due to the non-negligible population of the S = 0 ground state, confirming the presence of antiferromagnetic exchange interactions in all compounds.

Conclusions

This study involves the design of multidimensional transition-metal compounds with dcno$^-$ cyano carbanion acting as μ_2- and μ_3-bridging ligand. Previous work showed that reactions of the [(NC)$_2$CC(O)(OR)]$^-$ ligands (dcnm$^-$ for R = Me and dcne$^-$ for R = Et) with transition-metal ions afford 1D coordination polymers resulting from coordination of both ligands by their two nitrile groups.[11,12] A slight modification of the alkyl group leads us to the dnco$^-$ anion, for which the coordination modes in its metal ion binary systems strongly differ from those observed in the corresponding (dcnm)M and (dcne)M systems. However, as observed in the dcne$^-$ coordination polymers,[11] the highly conjugated [(NC)$_2$CC(O)O] group of the organic ligand precludes any localisation of the negative charge on the terminal oxygen atom and, therefore, its coordination to the metal centres. Thus, in the compounds [M(dcno)$_2$(H_2O)$_2$] [M = Fe^{II} (**1**), Co^{II} (**2**)], this anion acts as a μ_2 ligand, leading to 1D and 2D molecular arrangements respectively, while in the binary systems [M(dcno)$_2$] [M = Cu^{II} (**3**), Mn^{II} (**4**)] with the 3D networks, this anion acts as a μ_3 bridging ligand. This clearly illustrates the bonding affinity and flexibility of the cyanocarbanion ligand towards transition-metal ions. These unexpected structural differences can be partially explained by the less restricting coordination preferences of Cu^{II} (due to Jahn–Teller distortions) and Mn^{II} (due to its larger ionic radius). In contrast, in compounds **1** and **2** the dcno$^-$ ligand is not flexible enough to link the Fe^{II} and the Co^{II} ions through its terminal OH group (O3) as the metal–oxygen bonds should be shorter than the corresponding ones observed (and expected) for the Mn^{II} and Cu^{II} compounds [M–O distances observed in **1**–**4**: 2.141(3), 2.144(5), 2.359(2) and 2.197(2) Å, respectively]. This lack of flexibility induces the presence of water molecules in axial positions, leading to materials with low dimensionalities. In an effort to facilitate formation of 3D systems, syntheses of new parent cyanocarbanion ligands involving more flexible groups such as –O(CH_2)$_n$OH (n = 3, 4, …) are in progress.

Experimental Section

General: All reactions were performed under aerobic conditions. The reagents $AgNO_3$, $MnCl_2\cdot4H_2O$, $FeCl_2\cdot4H_2O$, $CoCl_2\cdot6H_2O$ and $CuCl_2\cdot2H_2O$ were purchased from commercial sources and used as received. 2-(1,3-Dioxolan-2-ylidene)malononitrile was prepared according to ref.[1g] IR spectra were recorded in the range 4000–200 cm^{-1} as KBr pellets with an FTIR NEXUS NICOLET Spectrometer. NMR spectra were recorded with a Bruker AMX 400 MHz instrument. Elemental analyses were obtained from the Service de microanalyses, CNRS, Gif sur Yvette, France. The magnetic studies were carried out on powder samples enclosed in medical caps. The magnetic susceptibility measurements were performed at 0.1 T, in the temperature range 2–300 K, with a SQUID magnetometer MPMS-XL-5 from Quantum Design. The molar susceptibility was corrected from the sample holder and diamagnetic contributions of all atoms (Pascal's tables).

Synthesis of the Silver Salt of 2,2-Dicyano-1-(2-hydroxyethoxy)-ethenolate [Ag(dcno)]: Silver 2,2-dicyano-1-(2-hydroxyethoxy)-ethenolate [Ag(dcno)] was prepared by smooth hydrolysis of 2-(1,3-dioxolan-2-ylidene)malononitrile in the presence of an excess of silver nitrate; the pH of the aqueous solution (initial value: 6.5) decreased to 1.0 after boiling the solution for a few minutes. An excess of $AgNO_3$ (4.077 g, 24 mmol) was added to a hot aqueous solution (30 mL) of 2-(1,3-dioxolan-2-ylidene)malononitrile (1.633 g, 12 mmol). The solution was stirred and heated until the solid dissolved. Slow concentration of the resulting solution at room temperature gave crystals of silver 2,2-dicyano-1-(2-hydroxyethoxy)-ethenolate as white needles (58% yield). $C_6H_5AgN_2O_3$ (260.99): calcd. C 27.6, H 1.9, Ag 41.3, N 10.7; found C 27.9, H 1.9, Ag 40.9, N 10.6. IR (KBr): $\tilde{\nu}$ = 3451 br, 2963 m, 2204 s, 2177 s, 1803 s, 1777 s, 1642 s, 1480 w, 1385 s, 1319 s, 1181 m, 1134 s, 1079 s, 975 m, 901 m, 824 m, 777 m, 755 m, 719 m, 553 m cm^{-1}. Because of the low solubility of this salt in most organic solvents, we prepared, by metathesis, its tetraethylammonium homologue by reaction of [Ag(dcno)] with 1 equiv. of $[(C_2H_5)_4N]Cl$ in CH_3CN in order to record the NMR spectrum and perform the IR study of the noncoordinated dcno⁻ anion. IR (KBr): $\tilde{\nu}$ = 3456 br, 2988 s, 2952 m, 2396 w, 2197 s, 2169 s, 1802 s, 1776 s, 1649 s, 1396 br, 1173 s, 1125 s, 1076 s, 1033 w, 1002 s, 974 w, 894 m, 825 m, 787 s, 756 m, 717 w, 555 m cm^{-1}. ^{13}C NMR ([D$_6$]acetone): δ = 170 [C(O)O], 123.7 (CN), 72.9 (CH_2), 65.4 (CH_2), 46.7 [$C(CN)_2$; 52.6, 7.4 $(C_2H_5)_4N$] ppm.

Syntheses of [M(dcno)$_2$(H$_2$O)$_2$] [M = Fe^{II} (1), Co^{II} (2)] and [M-(dcno)$_2$] [M = Cu^{II} (3), Mn^{II} (4)]: The four compounds were prepared in the same way by treating aqueous solutions (10 mL) of the corresponding metal chloride (1 mmol) with aqueous solutions (15 mL) of silver 2,2-dicyano-1-(2-hydroxyethoxy)ethenolate (2 mmol, 0.384 g). The samples were stirred at room temperature for about 30 min and left to stand. Slow concentration of the resulting solutions at room temperature gave prismatic crystals for compounds **1**–**4** that were filtered and air-dried. All compounds were satisfactory analysed for C, H and N. All compounds can also be prepared in the same way as the silver salts by direct reaction in aqueous solution of 2-(1,3-dioxolan-2-ylidene)malononitrile with the corresponding transition-metal salt, but this procedure does not allow the isolation of the pure dcno⁻ anion as the starting ligand and yields less pure compounds **1**–**4**, as the hydrolysis of the precursor is not complete.

1: Yield: 0.219 g (55%). $C_{12}H_{14}FeN_4O_8$ (398.11): calcd. C 36.2, H 3.5, N 14.1; found C 35.9, H 3.7, N 14.3. IR (KBr): $\tilde{\nu}$ = 3411 br, 3075 br, 2231 s, 2191 s, 1656 s, 1487 w, 1383 s, 1359 m, 1334 m, 1310 s, 1280 m, 1158 s, 1070 m, 1043 s, 986 w, 849 m, 815 m, 749 s, 585 w, 563 m cm^{-1}.

2: Yield: 0.233 g (58%). $C_{12}H_{14}CoN_4O_8$ (401.20): calcd. C 35.9, H 3.5, N 14.0; found C 35.6, H 3.6, N 14.3. IR (KBr): $\tilde{\nu}$ = 3411 br, 2250 s, 2215 s, 1623 s, 1457 w, 1437 w, 1392 m, 1326 s, 1284 m, 1265 w, 1171 s, 1075 m, 1013 w, 900 w, 758 w, 668 w, 553 w cm^{-1}.

3: Yield: 0.288 g (78%). $C_{12}H_{10}CuN_4O_6$ (369.78): calcd. C 39.0, H 2.7, N 15.2; found C 38.6, H 2.8, N 15.5. IR (KBr): $\tilde{\nu}$ = 3315 br, 2252 s, 2199 s, 1646 s, 1478 m, 1406 m, 1374 s, 1328 s, 1282 s, 1145 s, 1022 m, 810 w, 754 s, 556 s, 493 w, 431 m, 386 m cm^{-1}.

4: Yield: 0.173 g (48%). $C_{12}H_{10}MnN_4O_6$ (361.18): calcd. C 39.9, H 2.8, N 15.5; found C 40.3, H 2.6, N 15.2. IR (KBr): $\tilde{\nu}$ = 3401 br, 2232 s, 2196 s, 1650 s, 1615 s, 1460 m, 1400 s, 1383 m, 1285 w, 1229 w, 1160 s, 1087 m, 1070 m, 1020 w, 902 m, 758 m, 640 w, 558 m cm^{-1}.

X-ray Crystallography: Data for compounds **1**–**3** were collected with an Xcalibur 2 diffractometer (Oxford Diffraction) at room temperature (294 K for **1** and **2** and 288 K for **3**). The three structures were solved by direct methods and successive Fourier difference syntheses, and were refined, on *F*, by weighted anisotropic full-matrix least-squares methods.[21] The hydrogen atoms were located by difference Fourier map, except those of the "CH_2–CH_2" group of the dcno⁻ ligand in **1** and **2**, which were calculated [d(C–H) = 0.95 Å]; the thermal parameters were taken as $U_{iso} = 1.3U_{equ}(C)$ and therefore included as isotropic fixed contributors to F_c. Note

Table 2. Crystallographic data and structural refinement parameters for compounds **1**–**4**.

	1	**2**	**3**	**4**
Empirical formula[a]	$C_{12}H_{14}FeN_4O_8$	$C_{12}H_{14}CoN_4O_8$	$C_{12}H_{10}CuN_4O_6$	$C_{12}H_{10}MnN_4O_6$
Formula mass[a]	398.11	401.20	369.78	361.18
T [K]	294(2)	294(2)	288(2)	293(2)
Crystal system	monoclinic	orthorhombic	monoclinic	monoclinic
Space group	$C2/c$	$Pbca$	$P2_1/n$	$P2_1/n$
a [Å]	13.856(1)	9.952(1)	8.0521(3)	7.917(1)
b [Å]	7.450(1)	12.346(1)	8.9499(3)	9.114(2)
c [Å]	16.054(1)	13.587(1)	10.1242(4)	10.264(2)
β [°]	93.9(1)		96.5(1)	94.05(1)
V [Å^3]	1653.5	1669.3	724.9	738.8
$D_{calcd.}$ [g cm^{-3}]	1.60	1.60	1.69	1.62
Z[a]	4	4	2	2
μ [cm^{-1}]	9.57	10.71	15.44	9.31
Unique reflections/R_{int}	1745/0.052	1315/0.081	1995/0.03	14908
Reflections [$I > n\sigma(I)$]	909 (n = 2)	532 (n = 1.2)	1166 (n = 3)	14908 (n = 2)
N_v	126	115	106	127
R[b]	0.045	0.052	0.033	0.051
R_w[c]	0.048 (F_o)	0.056 (F_o)	0.037 (F_o)	0.152 (F_o^2)
Gof[d]	0.995	0.989	1.007	1.129
$\Delta\rho_{max}/\Delta\rho_{min}$ [e Å^{-3}]	+0.130/–0.239	+0.611/–0.513	+0.295/–0.600	+0.380/–0.287

[a] For all compounds the asymmetric unit contains 0.5 of the empirical formula. [b] $R = \Sigma||F_o| - |F_c||/\Sigma F_o|$. [c] $R_w(F_o) = \{\Sigma[w(F_o - F_c)^2]/\Sigma[w(F_o)^2]\}^{1/2}$; $R_w(F_o) = wR_2 = \{\Sigma[w(F_o^2 - F_c^2)^2]/\Sigma[w(F_o^2)^2]\}^{1/2}$. [d] Gof $= S = \{\Sigma[w(F_o^2 - F_c^2)^2]/(N_{obs} - N_{var})\}^{1/2}$.

that the hydrogen atoms of the water molecule and of the terminal "OH" group of the dcno$^-$ ligand in **2** were not calculated. It is noteworthy that it was difficult to collect correct X-ray data for compounds **1** and **2** because of their low diffracting power, essentially because of the low dimensions of the single crystals. However, the corresponding bond lengths and bond angles (see Table 1) are relatively correct, as they are in the normal range when compared to their corresponding values observed in the parent compounds **3** and **4**. For **4**, no pure single crystal was found. φ-χ scans performed on the KCCD diffractometer at 288 K and combined with the use of DIRAX program[22,23] revealed the existence of two misaligned crystal components with identical unit-cell parameters. Finally, the collected frames were integrated using the EVAL program considering both orientation matrices.[24] An HKLF5 file for the SHELX refinement program was created with a list of integrated intensities for the two observed contributors. For all integrated reflections, a reflection index specifying the quality of the reflection (pure #1, pure #2 or common reflection) was given. The structure was then solved by direct methods and successive Fourier difference syntheses, and was refined, on F^2, by weighted anisotropic full-matrix least-squares methods.[25] All the hydrogen atoms were located by difference Fourier map and were refined isotropically. In the least-square refinement procedure, a supplementary parameter defining the fractional contribution of the second component was refined. Note that because of the bicrystalline character of the studied object, the R_{int} parameter has no significance and so is not calculated by the refinement program. Scattering factors and corrections for anomalous dispersion were taken from the International Tables for X-ray Crystallography.[26] The thermal ellipsoid drawings were created with the ORTEP program.[27] Selected bond lengths and bond angles are listed in Table 1. Pertinent crystal data are mentioned in Table 2. CCDC-604823 to -604826 (for **1**–**4**, respectively) contain the supplementary crystallographic data for this paper. These data can be obtained free of charge from the Cambridge Crystallographic Data Centre via www.ccdc.cam.ac.uk/data_request/cif.

Acknowledgments

The authors gratefully acknowledge the Centre National de la Recherche Scientifique (CNRS) and the framework of a French–Spanish Integrated Action (PICASSO 2005/No. 07137XK and HF2003-258) for financial support. F. S. thanks the "Agence Universitaire pour la Francophonie" for a postdoctoral grant.

---

[1] a) O. W. Webster, W. Mahler, R. E. Benson, *J. Am. Chem. Soc.* **1962**, *84*, 3678–3684; b) L. R. Melby, R. J. Harder, W. R. Hertler, W. Mahler, R. E. Benson, W. E. Mochel, *J. Am. Chem. Soc.* **1962**, *84*, 3374–3387; c) T. L. Cairns, B. C. McKusick, *Angew. Chem.* **1961**, *73*, 520–525; d) W. J. Middleton, E. L. Little, D. D. Coffman, V. A. Engelhardt, *J. Am. Chem. Soc.* **1958**, *80*, 2775–2778; e) R. E. Merrifield, W. D. Phillips, *J. Am. Chem. Soc.* **1958**, *80*, 2778–2782; f) W. J. Middleton, R. E. Heckert, E. L. Little, C. G. Krespan, *J. Am. Chem. Soc.* **1958**, *80*, 2783–2788; g) W. J. Middleton, V. A. Engelhardt, *J. Am. Chem. Soc.* **1958**, *80*, 2788–2795; h) W. J. Middleton, E. L. Little, D. D. Coffman, V. A. Engelhardt, *J. Am. Chem. Soc.* **1958**, *80*, 2795–2809.

[2] a) K. R. Dunbar, *Angew. Chem.* **1996**, *108*, 1769–1771; *Angew. Chem. Int. Ed. Engl.* **1996**, *35*, 1659–1671; b) W. Kaim, M. Moscherosch, *Coord. Chem. Rev.* **1994**, *129*, 157–173; c) J. M. Manriquez, T. Y. Gordon, R. S. McLean, A. J. Epstein, J. S. Miller, *Science* **1991**, *252*, 1415–1417; d) R. Kato, H. Kobayashi, A. Kobayashi, *J. Am. Chem. Soc.* **1989**, *111*, 5224–5232; e) J. S. Miller, A. J. Epstein, W. M. Reiff, *Chem. Rev.* **1988**, *88*, 201–220.

[3] S. R. Batten, K. S. Murray, *Coord. Chem. Rev.* **2003**, *246*, 103–130 and references cited therein.

[4] a) M. R. Pederson, A. Y. Liu, T. Baruah, E. Z. Kurmaev, A. Moewes, S. Chiuzbaian, M. Neumann, C. R. Kmety, K. L. Stevenson, D. Ederer, *Phys. Rev. C: Nucl. Phys.* **2002**, *66*, 014446/1–014446/8; b) J. L. Manson, C. R. Kmety, F. Palacio, A. J. Epstein, J. S. Miller, *Chem. Mater.* **2001**, *13*, 1068–1073; c) C. R. Kmety, Q.-Z. Huang, J. W. Lynn, R. W. Erwin, J. L. Manson, S. McCall, J. E. Crow, K. L. Stevenson, J. S. Miller, A. J. Epstein, *Phys. Rev. B: Condens. Matter* **2000**, *62*, 5576–5588; d) S. R. Batten, P. Jensen, C. J. Kepert, M. Kurmoo, B. Moubaraki, K. S. Murray, D. J. Price, *J. Chem. Soc., Dalton Trans.* **1999**, 2987–2997; e) P. Jensen, S. R. Batten, G. D. Fallon, B. Moubaraki, K. S. Murray, D. J. Price, *Chem. Commun.* **1999**, 177–178; f) J. L. Manson, C. R. Kmety, A. J. Epstein, J. S. Miller, *Inorg. Chem.* **1999**, *38*, 2552–2553; g) S. R. Batten, P. Jensen, B. Moubaraki, K. S. Murray, R. Robson, *Chem. Commun.* **1998**, 439–440; h) M. Kurmoo, C. J. Kepert, *New J. Chem.* **1998**, *22*, 1515–1524; i) J. L. Manson, C. R. Kmety, Q. Z. Huang, J. W. Lynn, G. M. Bendele, S. Pagola, P. W. Stephens, L. M. Liable-Sands, A. L. Rheingold, A. J. Epstein, J. S. Miller, *Chem. Mater.* **1998**, *10*, 2552–2560.

[5] a) R. Feyerherm, A. Loose, J. L. Manson, *J. Phys.: Condens. Matter* **2003**, *15*, 663–673; b) J. L. Manson, E. Ressouche, J. S. Miller, *Inorg. Chem.* **2000**, *39*, 1135–1141; c) S. R. Batten, B. F. Hoskins, B. Moubaraki, K. S. Murray, R. Robson, *J. Chem. Soc., Dalton Trans.* **1999**, 2977–2986; d) H. Oshino, K. Iida, T. Kawamoto, T. Mori, *Inorg. Chem.* **1999**, *38*, 4229–4232; e) J. L. Manson, C. Campana, J. S. Miller, *Chem. Commun.* **1998**, 251–252; f) S. R. Batten, B. F. Hoskins, R. Robson, *New J. Chem.* **1998**, *22*, 173–175.

[6] P. Jensen, D. J. Price, S. R. Batten, B. Moubaraki, K. S. Murray, *Chem. Eur. J.* **2000**, *6*, 3186–3195.

[7] a) J. A. Schlueter, J. L. Manson, K. A. Hyzer, U. Geiser, *Inorg. Chem.* **2004**, *43*, 4100–4102; b) P. M. van der Werff, S. R. Batten, P. Jensen, B. Moubaraki, K. S. Murray, E. H. K. Tan, *Polyhedron* **2001**, *20*, 1129–1138; c) J. W. Raebiger, J. L. Manson, R. D. Sommer, U. Geiser, A. L. Rheingold, J. S. Miller, *Inorg. Chem.* **2001**, *40*, 2578–2581; d) P. M. van der Werff, S. R. Batten, P. Jensen, B. Moubaraki, K. S. Murray, *Inorg. Chem.* **2001**, *40*, 1718–1722; e) S. R. Batten, P. Jensen, B. Moubaraki, K. S. Murray, *Chem. Commun.* **2000**, 2331–2332.

[8] a) S. C. Manna, A. K. Ghosh, J. Ribas, M. G. B. Drew, C.-N. Lin, E. Zangrando, N. R. Chaudhuri, *Inorg. Chim. Acta* **2006**, *359*, 1395–1403; b) L. F. Jones, L. O'Dea, D. A. Offermann, P. Jensen, B. Moubaraki, K. S. Murray, *Polyhedron* **2006**, *25*, 360–372; c) J. Luo, Z.-H. Shao, E.-Q. Gao, C.-F. Wang, R.-F. Cai, X.-G. Zhou, *Inorg. Chem. Commun.* **2006**, *9*, 196–200; d) G.-Y. Hsu, C.-W. Chen, S.-C. Cheng, S.-H. Lin, H.-H. Wei, C.-J. Lee, *Polyhedron* **2005**, *24*, 487–494; e) C.-F. Hsu, S.-H. Lin, H.-H. Wie, *Inorg. Chem. Commun.* **2005**, *7*, 1128–1132; f) J. Luo, X.-G. Zhou, S. Gao, L.-H. Weng, Z.-H. Shao, C.-M. Zhang, Y.-R. Li, J. Zhang, R.-F. Cai, *Inorg. Chem. Commun.* **2004**, *7*, 669–672; g) J. L. Manson, J. A. Schlueter, *Inorg. Chim. Acta* **2004**, *357*, 3975–3979; h) J. L. Manson, J. A. Schlueter, H.-J. Koo, M.-H. Whangbo, *Inorg. Chem.* **2004**, *43*, 4007–4011.

[9] a) E. Colacio, I. Ben Mimoun, F. Lloret, J. Suárez-Varela, *Inorg. Chem.* **2005**, *44*, 3771–3773; b) O. V. Nesterova, S. R. Petrusenko, V. N. Kokozay, B. W. Skelton, W. Linert, *Inorg. Chem. Commun.* **2004**, *7*, 450–454; c) Z. M. Wang, B.-W. Sun, J. Luo, S. Gao, C.-S. Liao, C.-H. Yan, Y. Li, *Inorg. Chim. Acta* **2002**, *332*, 127–134.

[10] a) S. Triki, F. Thétiot, F. Vandevelde, J. Sala-Pala, C. J. Gómez-García, *Inorg. Chem.* **2005**, *44*, 4086–4093; b) F. Thétiot, S. Triki, J. Sala-Pala, S. Golhen, *Inorg. Chim. Acta* **2005**, *358*, 3277–3282; c) F. Thétiot, S. Triki, J. Sala-Pala, J. R. Galán-Mascarós, J. M. Martínez-Agudo, K. R. Dunbar, *Eur. J. Inorg.*

Chem. **2004**, 3783–3791; d) F. Thétiot, S. Triki, J. Sala-Pala, S. Golhen, *Inorg. Chim. Acta* **2003**, *350*, 314–320.

[11] F. Thétiot, S. Triki, J. Sala-Pala, C. J. Gómez-García, *J. Chem. Soc., Dalton Trans.* **2002**, 1687–1693.

[12] C. Kremer, C. Melián, J. Torres, M. P. Juanicó, C. Lamas, H. Pezaroglo, E. Manta, H. Schumann, J. Pickardt, F. Girgsdies, O. N. Ventura, F. Lloret, *Inorg. Chim. Acta* **2001**, *314*, 83–90.

[13] F. Thétiot, S. Triki, J. Sala-Pala, *Polyhedron* **2003**, *22*, 1837–1843.

[14] a) S. Triki, J. Sala-Pala, M. Decoster, P. Molinié, L. Toupet, *Angew. Chem.* **1999**, *111*, 155–158; *Angew. Chem. Int. Ed.* **1999**, *38*, 113–115; b) S. Triki, J. Sala-Pala, A. Riou, P. Molinié, *Synth. Met.* **1999**, *102*, 1472–1473.

[15] M. Decoster, J. E. Guerchais, Y. Le Mest, J. Sala-Pala, S. Triki, L. Toupet, *Polyhedron* **1996**, *15*, 195–202.

[16] A. B. Gaspar, M. C. Munoz, J. A. Real, *Inorg. Chem. Commun.* **2004**, *7*, 815–817.

[17] See, for example: R. March, W. Clegg, R. A. Coxall, L. Cucurull-Sánchez, L. Lezama, T. Rojo, P. González-Duarte, *Inorg. Chim. Acta* **2003**, *353*, 129.

[18] O. Kahn, *Molecular Magnetism*, VCH Publishers, New York, **1993**.

[19] M. E. Fisher, *Am. J. Phys.* **1964**, *32*, 343.

[20] M. E. Lines, *J. Phys. Chem. Solids* **1970**, *31*, 101.

[21] C. K. Fair, *MolEN, An Interactive Intelligent System for Crystal Structure Analysis*, User Manual, Enraf-Nonius, Delft, The Netherlands, **1985**.

[22] A. J. M. Duisenberg, R. W. W. Hooft, A. M. M. Schreurs, J. Kroon, *J. Appl. Crystallogr.* **2000**, *33*, 893–898.

[23] A. J. M. Duisenberg, *J. Appl. Crystallogr.* **1992**, *25*, 92–96.

[24] A. J. M. Duisenberg, L. M. J. Kroon-Batenburg, A. M. M. Schreurs, *J. Appl. Crystallogr.* **2003**, *36*, 220–229.

[25] G. M. Sheldrick, *SHELX97, Programs for Crystal Structure Analysis*, University of Göttingen, Göttingen, Germany, **1997**.

[26] *International Tables for X-ray Crystallography*, Kynoch Press, Birmingham, **1975**, vol. 4.

[27] C. K. Johnson, *ORTEP*, Rep. ONL-3794, Delft, The Netherlands, **1985**.

Received: May 13, 2006